Available online at www.sciencedirect.com

ScienceDirect

Procedia Engineering 189 (2017) 133 – 137

Procedia Engineering

www.elsevier.com/locate/procedia

Transportation Geotechnics and Geoecology, TGG 2017, 17-19 May 2017, Saint Petersburg, Russia

Modeling the dynamic behavior of the upper structure of the railway track

Alexey A.Loktev[a], Vadim V. Korolev[a], Irina V. Shishkina[a], Dmitrii A. Basovsky[b]*

[a]*Moscow State University of Railway Emperor Nicholas II (MIIT), Moscow, 125993, Russia*
[b]*Emperor Alexander I St. Petersburg State Transport University, Saint Petersburg, 190031, Russia*

Abstract

The present work is devoted to modeling the behavior of railway track under dynamic load of wheel pair in view of elastic, viscoelastic and elastic-plastic properties of the area of interaction between two solids and elastic anisotropic properties of the subgrade, which differ in three main areas: along the rails along the sleepers and vertically downwards. The wave equation railway tracks suggest that the deformation and the permanent way and the mound itself is the field of interaction of bodies takes place in view of the spread of a finite speed of the wave surfaces. The solution methods used methods of asymptotic expansions in the time and space coordinate, the method of matching the expansions obtained for short times in the contact zone and outside it.

Peer-review under responsibility of the scientific committee of the International conference on Transportation Geotechnics and Geoecology

Keywords: dynamic interaction, the condition of compatibility, railway embankment, engineering-geological factors, dynamic sag.

1. Introduction

to explore in detail the process of dynamic loading of the track structure with subsequent establishment of dependencies for buckling and stresses it is necessary to simulate the dependencies of the force of interaction on different types of deformation (including bearing deformation) [1-12]. The main approaches that allow the detailed modeling of the interaction process between two rigid bodies differ from one another in the force acting in the contact area [1-5] and the nature of motion of the track (rail) points outside of the interaction region [6-12].

* Corresponding author. Tel.: +7-909-994-14-44,+7-916-126-84-18, +7-916-646-45-78, +7-960-234-61-82
E-mail address: aaloktev@yandex.ru, korolevadim@mail.ru, shishkinaira@inbox.ru, d1976bas@rambler.ru

Peer-review under responsibility of the scientific committee of the International conference on Transportation Geotechnics and Geoecology
doi:10.1016/j.proeng.2017.05.022

After the beginning of the interaction of the wheel set, which is represented by a solid body and the construction of the top ways [13-16], the contact area with the radius of r_0 is formed in this construction and both the quasi-longitudinal and quasi-transverse waves [17-19], which fronts represent surfaces of strong discontinuity, start to propagate from its surface [20-22].

2. Governing equation for wave problem

The embankment of the railway is modeled by an elastic orthotropic two-dimensional Uflyand-Mindlin element that exhibits a cylindrical anisotropy. In the polar coordinate system, the dynamic behavior of this element is described using equations which take into account the rotary inertia of the cross sections, deformation of the transverse shear and axial symmetry of the problem [4]:

$$\frac{\partial^2\varphi}{\partial r^2}+\frac{1}{r}\frac{\partial\varphi}{\partial r}+\frac{1}{r^2}\frac{\partial^2\varphi}{\partial\theta^2}-\frac{1}{r^2}\frac{c_2}{c_1}\varphi+\frac{c_2\sigma_r+c_3}{c_1 r}\frac{\partial^2\psi}{\partial r\partial\theta}-\frac{c_2+c_3}{c_1 r^2}\frac{\partial\varphi}{\partial\theta}+\frac{12c_4}{c_1}\left(\frac{\partial w}{\partial r}-\varphi\right)=-\frac{\partial^2\varphi}{\partial\tau^2},$$

$$\frac{c_4}{c_1}\left(\frac{\partial^2 w}{\partial r^2}-\frac{\partial\varphi}{\partial r}\right)+\frac{c_4}{c_1}\left(\frac{\partial w}{r\partial r}-\frac{\varphi}{r}\right)+\frac{c_4}{c_1}\left(\frac{\partial^2 w}{r^2\partial\theta^2}-\frac{\partial\psi}{r\partial\theta}\right)=\frac{\partial^2 w}{\partial\tau^2}+q_1,$$

$$\left(\frac{\partial^2 u}{\partial r^2}+\frac{1}{r}\frac{\partial u}{\partial r}\right)+\frac{c_3}{c_1 r^2}\frac{\partial^2 u}{\partial\theta^2}-\frac{c_2}{c_1}\frac{u}{r^2}+\frac{c_2\sigma_r+c_3}{c_1 r}\frac{\partial^2 v}{\partial r\partial\theta}-\frac{c_2+c_3}{c_1 r^2}\frac{\partial v}{\partial\theta}=\frac{\partial^2 u}{\partial\tau^2}, \tag{1}$$

$$\frac{c_2}{c_1 r^2}\frac{\partial^2 v}{\partial\theta^2}+\frac{c_3}{c_1}\left(\frac{\partial^2 v}{\partial r^2}+\frac{1}{r}\frac{\partial v}{\partial r}-\frac{v}{r^2}\right)+\frac{\sigma_\theta+c_3}{c_1 r}\frac{\partial^2 u}{\partial r\partial\theta}+\frac{c_2+c_3}{c_1 r^2}\frac{\partial u}{\partial\theta}=\frac{\partial^2 v}{\partial\tau^2},$$

$$\frac{c_3}{c_1}\left(\frac{\partial^2\psi}{\partial r^2}+\frac{1}{r}\frac{\partial\psi}{\partial r}-\frac{\psi}{r^2}\right)+\frac{c_2}{c_1 r^2}\frac{\partial^2\psi}{\partial\theta^2}+\frac{\sigma_\theta+c_3}{c_1 r}\frac{\partial^2\varphi}{\partial r\partial\theta}+\frac{c_2+c_3}{c_1 r^2}\frac{\partial\varphi}{\partial\theta}+\frac{12c_5}{c_1}\left(\frac{1}{r}\frac{\partial w}{\partial\theta}-\psi\right)=-\frac{\partial^2\psi}{\partial\tau^2},$$

where $\tau=\frac{t\sqrt{c_1}}{h}$, $w=\frac{w}{h}$, $u=\frac{u}{h}$, $v=\frac{v}{h}$, $r=\frac{r}{h}$, $c_1=\frac{E_r}{(1-\sigma_r\sigma_\theta)\rho}$, $c_2=\frac{E_\theta}{(1-\sigma_r\sigma_\theta)\rho}$, $c_3=\frac{G_{r\theta}}{\rho}$, $c_4=\frac{KG_{rz}}{\rho}$,

$c_5=\frac{KG_{\theta z}}{\rho}$, $q_1=\frac{qh}{\rho c_1}$, $D_r=\frac{h^3}{12}B_r$, $D_\theta=\frac{h^3}{12}B_\theta$, $D_k=\frac{h^3}{12}B_k$, $C_r=hB_r$, $C_\theta=hB_\theta$, $C_k=hB_k$, $D_{r\theta}=D_r\sigma_\theta+2D_k$,

$B_r=\frac{E_r}{1-\sigma_r\sigma_\theta}$, $B_\theta=\frac{E_\theta}{1-\sigma_r\sigma_\theta}$, $B_k=G_{r\theta}$, $E_r\sigma_r=E_\theta\sigma_\theta$, $K=5/6$, D_r, D_θ and C_r, C_θ - the bending regidity and and tension-compresiion rigidity for r and θ directions, respectively; D_k – the torsional regidity; C_k – the shear stiffness; E_r, E_θ and σ_r, σ_θ - the coefficients of elastisity and Poisson's ratios for r and θ directions, respectively; G_{rz}, $G_{\theta z}$ – the shear modules for rz and θz planes, respectively; $w(r,\theta)$ – the normal displacement of the median plane, $u(r,\theta)$ and $v(r,\theta)$ – the tangential displacements of the medial surface with respect to r and θ coordinates; $\varphi(r,\theta)$ and $\psi(r,\theta)$ – the rotation angles of the normals in r and θ directions r,θ (fig.1), ρ - density, q – load, R_1 – radius of spherical impactor, h – thickness of the plate.

To determine the unknown displacements in Eq. (1) the following series expansion can be used [2,4,5,6]:

$$Z(s,t)=\sum_{k=o}^{\infty}\frac{1}{k!}\left[Z_{,(k)}\right]_{t=s/G}\left(t-\frac{s}{G}\right)^k H\left(t-\frac{s}{G}\right), \tag{2}$$

where Z – the required function, $Z_{,(k)}={}^kZ/t^k$, , the upper indices «+» and «-» of the derivative $Z_{,(k)}$ indicate that the value is found in front of and behind the wave surface, respectively, G – the normal velocity of the wave, $H(t\text{-}s/G)$ – the Heaviside step function, s – length of a curve, measured along the ray, t – time.

The proposed method is based on the applying the geometric and kinematic conditions of compatibility, suggested in reference [1] and developed for physical components in the paper [2] as follows:

$$G\left[\frac{\partial Z_{\gamma(k)}}{\partial s}\right]=-\left[Z_{\gamma(k+1)}\right]+\frac{\delta\left[Z_{\gamma(k)}\right]}{\delta t}, \tag{3}$$

where $\delta/\delta t$ - δ-time-derivative at the surface of the wavefront.

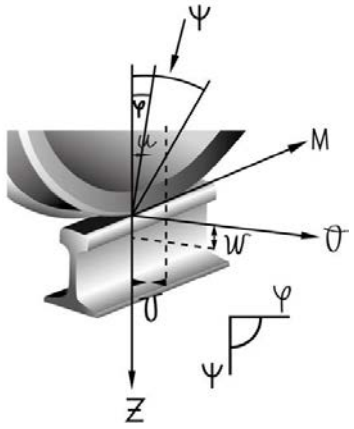

Fig. 1. Model of the contact between wheel and rail.

3. Contact problem

To determine the coefficients of the series (2) for the required functions it is necessary to differentiate the wave equations (1) *k* times with respect to time, calculate their difference at various sides of the wave surface and apply the compatibility condition (3). The found discontinuities allow one to write the expressions for the required functions in a view of an interval of the ray series within the accuracy of the coefficients, which are determined from the boundary conditions [2,4,5,13]. In order to determine the integration constants it is required to consider the problem of a dynamic contact between the wheel set and the track structure [9,10,11,15]. For the modelling of the contact the buffer is used, which can be represented as an elastic, visco-elastic and elastic-plastic element. For these three elements the dependencies of the arising contact force in the point of interaction on the rail displacement and mechanic characteristics of applied materials are determined [2,3,4,5,6,18]

$$P(t)=E_1\left(a(t)-w(t)\right), \tag{4}$$

$$P(t)=E_1(\alpha-w)-\frac{E_1}{\tau_1}\int_0^t(\dot{\alpha}-\dot{w})e^{-\frac{t-t'}{\tau_1}}dt', \tag{5}$$

$$\alpha=\begin{cases} bP^{2/3}, & dP/dt>0,\ P_{\max}<P_1,\\ (1+\beta)c_1+(1-\beta)Pd, & dP/dt>0,\ P_{\max}>P_1,\\ b_fP^{2/3}+\alpha_p(P_{\max}), & dP/dt<0,\ P_{\max}>P_1, \end{cases} \tag{6}$$

$$\alpha=\begin{cases} bP^{2/3}, & dP/dt>0,\ P<P_b,\\ bP^{2/3}+Pd, & dP/dt>0,\ P>P_b,\\ bP^{2/3}+P_{\max}d, & dP/dt<0,\ P_{\max}>P_b, \end{cases} \tag{7}$$

where $b=\left(\left(9\pi^2(k_1+k)^2\right)/16R\right)^{1/3}$, $k_1=\left(1-\sigma_1^2\right)/E_1$, $k=\left(1-\sigma^2\right)/E$, $P_1=\chi^3\left(3R(k_1+k)/4\right)^2$, λ=5.7,

$b_f=R_f^{-1/3}\left(3(k_1+k)/4\right)^{2/3}$, $R_p^{-1}=R^{-1}-R_f^{-1}$, $R_f=\left(4/3(k_1+k)\right)P_{\max}^{1/2}\chi^{-3/2}$, $\alpha_p(P_{\max})=(1-\beta)P_{\max}\left(2\chi R_p\right)^{-1}$,

$c_1 = 3\chi^{1/2}(k_1 + k)/8$, $\beta = 0.33$, $d = 1/2\chi R$, $\chi = \pi k_{pl}\lambda$, k_{pl} – the minimal plastic constant of the interacting bodies, σ_1, E_1 – the Poisson's ratio and the module of rigidity of the wheel set, respectively, $\tau_1 = \eta_1/E_1$, τ_1 – the relaxation time in the case of the visco-elastic model, t' - the integration variable, η_1 – the viscosity coefficient, α, w - displacements of the upper and lower ends of the rail, respectively.

4. Splicing solutions contact and wave problems

For the determination of the integration constants it is necessary to write a system of equations that describes the behavior of the wheel set, the buffer and the rail contact area after the biginning of the interaction [4,5,8,9].

Taking into account the condition of a horizontal position of the tangent line towards the middle surface of the rail at the boundary points of the contact area with the wheel set, the system of equations defining the process of interaction between the wheel, rail and tie may be obtained [9,10,18]. This system is solved using the following initial conditions:

$$\dot{w}\big|_{t=0} = 0, \quad \dot{\alpha}\big|_{t=0} = V_0.$$

By solving the system of equations, which determine the behavoir of the interacting bodies after the beginning of the contact, at equal times and based on Eq. (4) the expression for the interaction force between the wheel and the rail my be written as

$$P(t) = E_1 V_0 \left[t - E_1 \left(\frac{1}{m} + \frac{2}{\rho h \pi r_0^2} \right) \frac{t^3}{6} + \frac{E_1 \left(G^{(1)} + G^{(2)} \right)}{\rho h \pi r_0^3} \frac{t^4}{6} - E_1 \left[\frac{\left(G^{(1)} + G^{(2)} \right)^2}{\rho h \pi r_0^4} - \frac{E_1}{6} \left(\frac{1}{m} + \frac{2}{\rho h \pi r_0^2} \right)^2 \right] \frac{t^5}{20} + \right.$$

$$+ E_1 \left[- \frac{4E_1 \left(G^{(1)} + G^{(2)} \right)}{\rho h \pi r_0^3} \left(\frac{1}{m} + \frac{2}{\rho h \pi r_0^2} \right) + \frac{4\left(G^{(1)} + G^{(2)} \right)^3}{\rho h \pi r_0^5} - \right. \tag{8}$$

$$\left. \left. - \frac{1}{4} \frac{\left(G^{(1)3} + G^{(2)3} \right)}{\rho h \pi r_0^5} - \frac{12}{\rho h^3 \pi r_0^2} \frac{\left(G^{(1)3} - G^{(2)3} \right) G^{(2)2}}{G^{(1)2} - G^{(2)2}} + \frac{1}{\rho h \pi r_0^5} \left(\frac{E_\theta}{E_r} - 1 \right) \frac{G^{(1)3} G^{(2)}}{G^{(1)} - G^{(2)}} \right] \frac{t^6}{360} \right].$$

Figure 2 shows the time dependencies of the dimensionless contact force for different interaction models: curve 1 – elastic contact (Eq. (4)), curve 2 – visco-elastic contact (Eq. (5)), curve 3 – elastoplastic contact (Eq. (6)). The dotted line depicts the results of the experimental tests, carried out using a geometry car. From Fig. 2 it can be seen that the elastic model (Eq. (4)) gives the best approximation to the experimentally obtained data in respect to the maximal force value, the contact time and type of a graphic dependence.

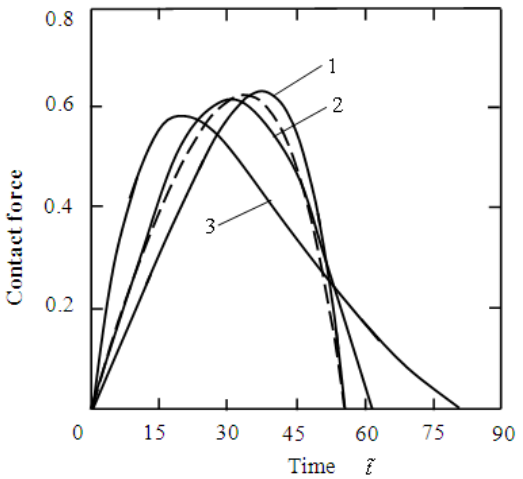

Fig.2. The dependence of the force of interaction on time for different models of contact.

5. Conclusion

The conducted investigations have shown that the elastic model describes in the best way the behavior of the force in the point of interaction and by correctly choosing the stiffness properties of the superstructure and the main body of the embankment allows for the precise determination of the railway behavior with the dynamic loading. Operating by a kinematic parameter and a power parameter it is possible to find such a velocity and a cargo regime of the wagonage passing, at which the railway track would be less destroyed. On the contrary, by knowing the parameters of the velocity and the pressure on the axis one can determine the suitable materials for the embankment and the underlayer, as well as the parameters of armoring of the grade level, at which the arising sag and stresses would not exceed the acceptable value.

References

[1] T.Y. Thomas, Plastic Flow and Fracture in Solids. N.Y. L.:Acad. Press, 1961.
[2] Yu.A. Rossikhin, M.V. Shitikova, A ray method of solving problems connected with a shock interaction 102, 1-4 (1994) 103-121.
[3] D.G. Birukov, I.G. Kadomtsev, Dynamic elastoplastic contact of an indenter and a spherical shell. Prikl. Mekh Tech. Phys. 43 (2002) 171–175 [in Russian]
[4] A.A. Loktev, E.A. Gridasova, E.V. Zapol'nova Simulation of the Railway under Dynamic Loading. Part 1. Ray Method for Dynamic Problem, Contemporary Engineering Sciences, 8,18 (2015) 799 – 807
[5] A.A. Loktev, E.A. Gridasova, A.V. Sycheva and R.N. Stepanov, Simulation of the Railway under Dynamic Loading. Part 2. Splicing Method of the Wave and Contact Solutions, Contemporary Engineering Sciences, 8, 21 (2015) 955 – 962
[6] J.D. Achenbach, D.P. Reddy, Note on wave propagation in linear viscoelastic media, Z. Angew. Math. Phys. 18 (1967) 141-144.
[7] S. Abrate, Modelling of impact on composite structures, Composite Structures. 51 (2001) 129-138.
[8] R. Olsson , M.V. Donadon , B.G. Falzon, Delamination threshold load for dynamic impact on plates, International Journal of Solids and Structures. 4 3 (2006) 3124-3141.
[9] R. Tiberkak , M. Bachene , S. Rechak , B. Necib, Damage prediction in composite plates subjected to low velocity impact, Composite Structures. 83 (2008) 73-82.
[10] M. Agostinacchio, D. Ciampa, M. Diomedi, S. Olita, Parametrical analysis of the railways dynamic response at high speed moving loads, Journal of Modern Transportation. 21, 3 (2013) 169 – 181.
[11] A.A. Loktev, E.A. Gridasova, & V.V. Kramchaninov, The Method of Determining the locations of reinforcing elements in a composite orthotropic plate undergoing dynamic impact. Part 1. Wave problem. Applied Mathematical Sciences. 9,71 (2015) 3533 – 3540
[12] A.A. Loktev, Dynamic contact of a spherical indenter and a prestressed orthotropic Uflyand-Mindlin plate. Acta Mechanica, 222, 1-2 (2011) 17-25.
[13] S. Abrate, Localized impact on sandwich structures with laminated facing. Applied Mechanics Reviews. 50, 2 (1997) 69-82.
[14] S. Abrate, Impact on laminated composite materials. Applied Mechanics Reviews. 44,4 (1991) 155-190.
[15] P. Chen, J. Xiong, Z. Shen, Thickness effect on the contact behavior of a composite laminate indented by a rigid sphere. Mechanics of Materials. 40 (2008) 183-194.
[16] A.P. Christoforou, A.A. Elsharkawy, L.H. Guedouar, An inverse solution for low-velocity impact in composite plates. Computers and Structures. 79 (2001) 2607-2619.
[17] V.N. Kukudzjanov, Investigation of shock wave structure in elasto-visco-plastic bar using the asymptotic method. Archive of Mechanics. 33, 5 (1981) 739-751.
[18] G.R. Evans, B.C. Jones, A.J. McMillan, M.I. Darby, A new numerical method for the calculation of impact forces. Journal of Physics D: Applied Physics. 24,6 (1991) 854-858.
[19] H.D. Fisher, The impact of an elastic sphere on a thin elastic plate supported by a Winkler foundation. Transactions of the ASME. Journal of Applied Mechanics. 42,1 (1975) 133-135.
[20] J. Jaeger, Analytical solutions of contact impact problems. Applied Mechanics Reviews. 47,2 (1994) 35-44.
[21] G.M. Shakhunyants, Calculations of the top structure of railway track. Moscow, Transzheldorizdat. 1959 [in Russian]
[22] A.Ya. Kogan, Calculations of rail track vertical dynamic load. Trudy VNIIZHT, 502, 80 p. 1973 [in Russian]